B_s Mixing at DØ

J. Walder[a] on behalf of the DØ Collaboration

[a]Lancaster University, Department of Physics, Lancaster, LA1 4YB, UK

The first direct two-sided bound by a single experiment on the B_s^0 oscillation frequency is reported using a sample of semileptonic decays collected between 2002 – 2006 by the Run IIa DØ detector at Fermilab, corresponding to approximately $1\,\text{fb}^{-1}$ of integrated luminosity. The most probable value of the oscillation frequency Δm_s is found from a likelihood scan to be 19 ps^{-1} and within the range $17 < \Delta m_s < 21$ ps^{-1} at the 90% C.L. At the preferred value of 19 ps^{-1} there is a 2.5σ deviation from a zero amplitude hypothesis.

This proceedings reports on an analysis of Bs mixing recently published in [1]. The phenomenon of particle anti-particle oscillations (or mixing) have provided insights into energy scales that had not yet been accessible. For example mixing in the neutral kaon system led to the prediction of a third flavour generation [2], and oscillations in the B_d^0 system gave predictions of the top quark mass [3]. Measuring the oscillation of the B_s^0 mixing frequency places a constraint on the magnitude of the CP violating top quark coupling from the ratio $|V_{td}/V_{ts}|$ and will perhaps yield a new physics discovery in $b \to s$ transitions [4]. Prior to this analysis, and assuming the Standard Model (SM) is correct, global fits to the unitarity triangle favoured $\Delta m_s = 20.9^{+4.5}_{-4.2}$ ps^{-1} [5]. This analysis was performed using a data sample of semileptonic B_s^0 decays collected with the DØ detector at Fermilab using $p\bar{p}$ collisions at $\sqrt{s} = 1.96$ TeV corresponding to an integrated luminosity of approximately 1 fb^{-1}.

The B_s^0 system can be described by the matrix evolution equation:

$$i\frac{d}{dt}\begin{pmatrix} B_s^0 \\ \bar{B}_s^0 \end{pmatrix} = \begin{pmatrix} M - \frac{i\Gamma}{2} & M_{12} - \frac{i\Gamma_{12}}{2} \\ M_{12}^* - \frac{i\Gamma_{12}^*}{2} & M - \frac{i\Gamma}{2} \end{pmatrix}\begin{pmatrix} B_s^0 \\ \bar{B}_s^0 \end{pmatrix}.$$

The two mass eigenstates differ from the flavour eigenstates and are defined as the eigenvectors of the above matrix. The heavy (H) and light (L) mass eigenstates are given by $|B_s^H\rangle = p|B_s^0\rangle + q|\bar{B}_s^0\rangle$, $|B_s^L\rangle = p|B_s^0\rangle - q|\bar{B}_s^0\rangle$, where $|p|^2 + |q|^2 = 1$. Denoting $\Delta m_s = M_H - M_L$, $\Delta\Gamma_s = \Gamma_L - \Gamma_H$, $\Gamma = (\Gamma_H + \Gamma_L)/2$, the probability for an initial B_s^0 meson at production to oscillate into a $\bar{B}_s^0$ (or vice-versa) at time t is given by $P^{\text{osc}} = \Gamma e^{-\Gamma t}(1 - \cos\Delta m_s t)/2$, or to not oscillate with probability $P^{\text{nosc}} = \Gamma e^{-\Gamma t}(1 + \cos\Delta m_s t)/2$, assuming $\Delta\Gamma_s/\Gamma_s$ is small and neglecting CP violation.

The DØ detector is a general purpose spectrometer and calorimeter [6]. The significant components for this analysis are the muon chambers, calorimeters and central tracking region. Enclosed within a 2 T superconducting solenoid is a silicon micostrip tracker (SMT) and central fiber tracker (CFT) for vertexing and tracking of charged particles that extends out to a pseudorapidity of $|\eta| = 2.0$, $\eta = -\ln[\tan(\theta/2)]$, where θ is the polar angle. The three liquid-argon/uranium calorimeters provide coverage up to $|\eta| \approx 4.0$. The muon system consists of one tracking layer and scintillation trigger counters in front of 1.8 T iron toroids with two layers after the toroids. Coverage extends to $|\eta| = 2.0$. There a no explicit trigger requirements used in this analysis, however most events were collected using single-muon triggers.

B_s^0 hadrons are selected using the semileptonic decay[1] $B_s^0 \to \mu^+\nu D_s^- X$, where $D_s^- \to \phi\pi^-$, $\phi \to K^+K^-$. The muon required a transverse momentum $p_T(\mu^+) > 2$ GeV/c, $p(\mu^+) > 3$ GeV/c, and to have a signal in at least two of layers of the muon system. All charged tracks in

[1]Charge conjugate states are implied throughout.

the event are required to have at least two signals in both the CFT and SMT and are clustered into jets [7]. The D_s^- candidate is reconstructed from three charged tracks in the same jet as the muon. Two oppositely charged particles with $p_T > 0.7$ GeV/c are assigned the mass of a kaon, and required to have an invariant mass $1.004 < M(K^+K^-) < 1.034$ GeV/c^2, consistent with a ϕ meson. The third track with charge opposite to that of the muon, and $p_T > 0.5$ GeV/c was assigned the mass of a pion. The three tracks are combined to form a common D_s^- vertex as described in Ref. [8]. This vertex was required to have a positive displacement relative to the $p\bar{p}$ collision point (PV), with a significance of at least 4σ. and $\cos(\alpha) > 0.9$, where α is the angle between the D_s^- momentum and the direction from the PV to the D_s^- vertex. The muon and D_s^- candidates are required to originate from a common B_s^0 vertex and have an invariant mass of the $\mu^+ D_s^-$ system between 2.6 and 5.4 GeV/c^2.

A likelihood ratio method [9] was utilised to increase the B_s^0 selection efficiency using the discriminating variables: the helicity angle between the D_s^- and $K^\pm$ momenta in the ϕ center-of-mass frame; isolation of the $\mu^+ D_s^-$ system; χ^2 of the D_s^- vertex; invariant masses $M(\mu^+ D_s^-)$ and $M(K^+K^-)$; and transverse momentum $p_T(K^+K^-)$. Sideband (B) and sideband-subtracted signal (S) $M(K^+K^-\pi)$ data distributions were used to construct the probability distribution functions (*pdf*s) for the discriminants. The combined likelihood selection variable was defined to maximise the predicted ratio $S\sqrt{S+B}$.

Following these requirements the number of D_s^- candidates was $N_{\rm tot} = 26{,}710 \pm 556\,({\rm stat})$, as shown in Fig. 1(a).

The flavour of the signal B_s^0 meson at production was determined using a likelihood ratio method using properties of the opposite-side b-hadron produced in the event. The performance of the opposite-side flavour tagger (OST) [10] is characterized by the efficiency $\epsilon = N_{\rm tag}/N_{\rm tot}$, where $N_{\rm tag}$ is the number of tagged B_s^0 mesons; tag purity η_s, defined as $\eta_s = N_{\rm cor}/N_{\rm tag}$, where $N_{\rm cor}$ is the number of B_s^0 mesons with correct flavour identification; and the dilution $\mathcal{D}$, related

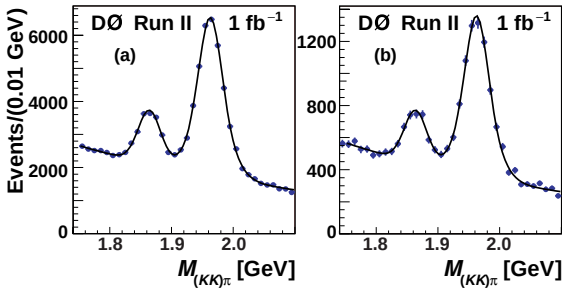

Figure 1. $(K^+K^-)\pi^-$ invariant mass distribution for (a) the untagged B_s^0 sample, and (b) for candidates that have been flavour-tagged. The left and right peaks correspond to $\mu^+ D^-$ and $\mu^+ D_s^-$ candidates, respectively. The curve is a result of fitting a signal plus background model to the data.

to purity as $\mathcal{D} \equiv 2\eta_s - 1$. A reconstructed secondary vertex or lepton ℓ (electron or muon) was defined to be on the opposite side of the B_s^0 meson if $\cos\varphi(\vec{p}_{\ell\ {\rm or\ SV}}, \vec{p}_B) < 0.8$, where $\vec{p}_B$ is the reconstructed three-momentum of the B_s^0 meson, and φ is the azimuthal angle about the beam axis. A lepton jet charge was formed as $Q_J^\ell = \sum_i q^i p_T^i / \sum_i p_T^i$, where all charged particles are summed, including the lepton, inside a cone of $\Delta R = \sqrt{(\Delta\varphi)^2 + (\Delta\eta)^2} < 0.5$ centered on the lepton. The SV charge was defined as $Q_{\rm SV} = \sum_i (q^i p_L^i)^{0.6} / \sum_i (p_L^i)^{0.6}$, where all charged particles associated with the SV are summed, and p_L^i is the longitudinal momentum of track i with respect to the direction of the SV momentum. Finally, event charge is defined as $Q_{\rm EV} = \sum_i q^i p_T^i / \sum_i p_T^i$, where the sum is over all tracks with $p_T > 0.5$ GeV/c outside a cone of $\Delta R > 1.5$ centered on the B_s^0 direction. The *pdf* of each discriminating variable was found for b and $\bar{b}$ quarks using a large data sample of $B^+ \to \mu^+ \nu \bar{D}^0$ events where the initial state is known from the charge of the decay muon. The likelihood ratio is parameterised to provide an event by event prediction of b quark. The OST purity was determined from large samples of non-oscillating $B^+ \to \mu^+ \bar{D}^0 X$ and oscillating $B_d^0 \to \mu^+ D^{*-} X$ semileptonic candidates. An average

value of $\epsilon\mathcal{D}^2 = [2.48 \pm 0.21\,(\text{stat})^{+0.08}_{-0.06}\,(\text{syst})]\%$ was obtained [10]. The OST was applied to the $B_s^0 \to \mu^+ D_s^- X$ data sample, yielding $N_{\text{tag}} = 5601 \pm 102\,(\text{stat})$ candidates having an identified initial state flavour, as shown in Fig. 1(b). The tagging efficiency was $(20.9 \pm 0.7)\%$.

Due to non-reconstructed particles in the event such as the neutrino, the measured proper decay length is smeared out and introduces resolution effects. A correction factor K was estimated from a Monte Carlo (MC) simulation by finding the distribution of $K = p_T(\mu^+ D_s^-)/p_T(B)$ for a given decay channel in bins of $M(\mu^+ D_s^-)$. The proper decay length of each B_s^0 meson is then $ct(B_s^0) = l_M K$, where $l_M = M(B_s^0) \cdot (\vec{L}_T \cdot \vec{p}_T(\mu^+ D_s^-))/(p_T(\mu^+ D_s^-))^2$ is the measured visible proper decay length (VPDL), $\vec{L}_T$ is the vector from the PV to the B_s^0 decay vertex in the transverse plane and $M(B_s^0) = 5.3696$ GeV/c^2 [11].

All flavour-tagged events with $1.72 < M(K^+K^-\pi^-) < 2.22$ GeV/c^2 were used in an unbinned fitting procedure. The likelihood, $\mathcal{L}$, for an event to arise from a specific source in the sample depends event-by-event on l_M, its uncertainty σ_{l_M}, the invariant mass of the candidate $M(K^+K^-\pi^-)$, the predicted dilution $\mathcal{D}(d_{\text{tag}})$, and the selection variable y_{sel}. Four sources were considered: the signal $\mu^+ D_s^-(\to \phi\pi^-)$; the accompanying peak due to $\mu^+ D^-(\to \phi\pi^-)$; a small (less than 1%) reflection due to $\mu^+ D^-(\to K^+\pi^-\pi^-)$, where the kaon mass is misassigned to one of the pions; and combinatorial background. The total fractions of the first two categories were determined from the mass fit of Fig. 1(b).

The signal sample of $\mu^+ D_s^-$ candidates consists mainly of B_s^0mesons with some contribution from B^0 and B^+ mesons with any b-baryon contribution estimated to be small and is neglected. The distribution of the VPDl l for non-oscillated and oscillated subsamples as determined by the OST is modelled for each type of B meson, e.g. for B_s^0:

$$p_s^{\text{nos/osc}}(l, K, d_{\text{tag}}) = \frac{K}{c\tau_{B_s^0}} \exp(-\frac{Kl}{c\tau_{B_s^0}}) \left[1 \pm \mathcal{D}(d_{\text{tag}}) \cos(\Delta m_s \cdot Kl/c)\right]/2. \quad (1)$$

The world averages [11] of $\tau_{B_d^0}$, τ_{B^+}, and Δm_d were used as inputs to the fit. The lifetime, $\tau_{B_s^0}$, was allowed to float in the fit. In the amplitude and likelihood scans described below, $\tau_{B_s^0}$ was fixed to this fitted value.

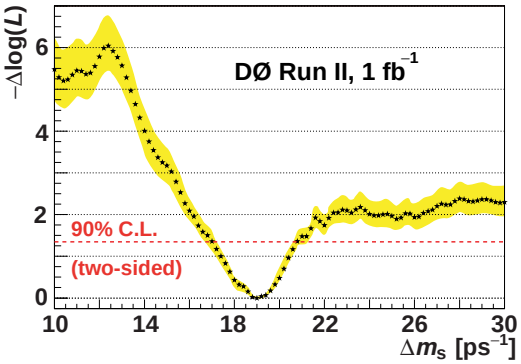

Figure 2. Value of $-\Delta \log \mathcal{L}$ as a function of Δm_s. Star symbols do not include systematic uncertainties, and the shaded band represents the envelope of all $\log \mathcal{L}$ scan curves due to different systematic uncertainties.

The total VPDL *pdf* for the $\mu^+ D_s^-$ signal is then the sum over all decay channels, including branching fractions, that yield the D_s^- mass peak. Backgrounds considered were decays via $B_s^0 \to D_{(s)}^+ D_s^- X$ and $\bar{B}_d^0, B^- \to D D_s^-$, followed by $D_{(s)}^+ \to \mu^+ X$, with a real D_s^- reconstructed in the peak and an associated real μ^+. Another background taken into account occurs when the D_s^- meson originates from one b or c quark and the muon arises from another quark.

Several contributions to the combinatorial backgrounds that have different VPDL distributions were considered. True prompt background was modeled with a Gaussian function with a separate scale factor on the width; background due to fake vertices around the PV was modeled with another Gaussian function; and long-lived background was modeled with an exponential function convoluted with the resolution, including a component oscillating with a frequency of Δm_d. The unbinned fit of the total tagged sample was used to determine the various fractions of signal and backgrounds and the background VPDL parametrizations.

Figure 2 shows the value of $-\Delta \log \mathcal{L}$ as a function of Δm_s, indicating a prefered value of

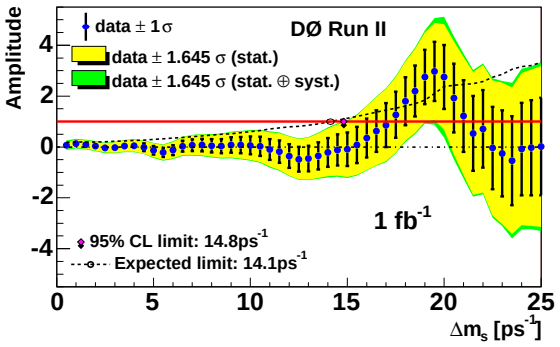

Figure 3. B_s^0 oscillation amplitude as a function of oscillation frequency, Δm_s. The solid line shows the $\mathcal{A} = 1$ axis for reference. The dashed line shows the expected limit including both statistical and systematic uncertainties.

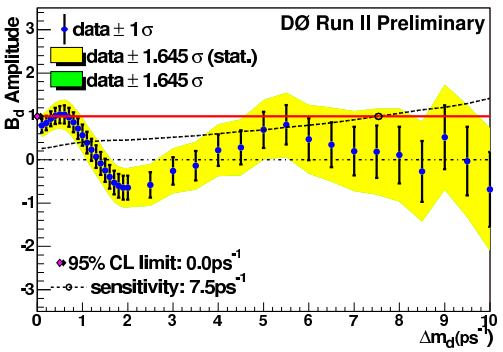

Figure 4. B_d^0 oscillation amplitude with statistical uncertainty only for events in the D^-mass region in Fig. 1 The red (solid) line shows the $A = 1$ axis for reference. The dashed line shows the expected limit including statistical uncertainties only.

19 ps^{-1}, while variation of $-\log\mathcal{L}$ from the minimum indicates an oscillation frequency of $17 < \Delta m_s < 21$ ps^{-1} at the 90% C.L. The uncertainties are approximately Gaussian inside this interval. For a true value $\Delta m_s > 22$ ps^{-1} there is insufficient resolution to measure an oscillation. From MC samples with similar statistics, VPDL resolution, overall tagging performance, and sample composition of the data sample, it was determined that for a true value of $\Delta m_s = 19$ ps^{-1}, the probability was 15% for measuring a value in the range $16 < \Delta m_s < 22$ ps^{-1} with a $-\Delta\log\mathcal{L}$ lower by at least 1.9 than the corresponding value at $\Delta m_s = 25$ ps^{-1}.

The amplitude method [12] was also used. Equation 1 was modified to include the oscillation amplitude $\mathcal{A}$ as an additional coefficient on the $\cos(\Delta m_s \cdot Kl/c)$ term. The unbinned fit was repeated for fixed input values of Δm_s and the fitted value of $\mathcal{A}$ and its uncertainty $\sigma_{\mathcal{A}}$ found for each step, as shown in Fig. 3. At $\Delta m_s = 19$ ps^{-1} the measured data point deviates from the hypothesis $\mathcal{A} = 0$ ($\mathcal{A} = 1$) by 2.5 (1.6) standard deviations, corresponding to a two-sided C.L. of 1% (10%), and is in agreement with the likelihood results. In the presence of a signal, however, it is more difficult to define a confidence interval using the amplitude than by examining the $-\Delta\log\mathcal{L}$ curve. Since, on average, these two methods give the same results, we chose to quantify our Δm_s interval using the likelihood curve. A cross-check of the B_s^0 analysis was performed using B^0 decays and Figure 4 shows a peak in the amplitude scan at a value $\Delta m_d \approx 0.5$ps^{-1}, compatible with the world average.

Systematic uncertainties were addressed by varying inputs within their range of uncertainties. Uncertainties included: cut requirements, *pdf* modelling, K-factor distributions, peaking and combinatorial backgrounds fractions, and refection contributions. The functional form to determine the dilution $\mathcal{D}(d_{\rm tag})$ was varied. The lifetime $\tau_{B_s^0}$ was fixed to its world average value, and $\Delta\Gamma_s$ was allowed to be non-zero. The scale factors on the signal and background resolutions were varied within uncertainties, and typically generated the largest systematic uncertainty in the region of interest. A separate scan of $-\Delta\log\mathcal{L}$ was taken for each variation, and the envelope of all such curves is indicated as the band in Fig. 2. The same systematic uncertainties were considered for the amplitude method using the procedure of Ref. [12], and, when added in quadrature with the statistical uncertainties, represent a small effect, as shown in Fig. 3. Taking these systematic un-

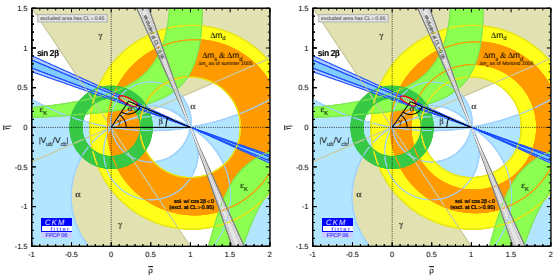

Figure 5. CKMFitter [13] plots of $(\bar{\rho}, \bar{\eta})$ plane with inputs as of FPCP 2006, excluding (left) and including (right) the result from this analysis.

certainties into account, we obtain from the amplitude method an expected limit of 14.1 ps^{-1} and an observed lower limit of $\Delta m_s > 14.8$ ps^{-1} at the 95% C.L., consistent with the likelihood scan.

The probability that B_s^0-$\bar{B}_s^0$ oscillations with the true value of $\Delta m_s > 22$ ps^{-1} would give a $-\Delta \log \mathcal{L}$ minimum in the range $16 < \Delta m_s < 22$ ps^{-1} with a depth of more than 1.7 with respect to the $-\Delta \log \mathcal{L}$ value at $\Delta m_s = 25$ ps^{-1}, corresponding to our observation including systematic uncertainties, was found to be (5.0 ± 0.3)%. This range of Δm_s was chosen to encompass the world average lower limit and the edge of our sensitive region. This probability was determined by randomly assigning a flavour to each candidate, effectively simulating a B_s^0 oscillation with an infinite frequency.

To summarise, a study of B_s^0-$\bar{B}_s^0$ oscillations was performed using $B_s^0 \to \mu^+ D_s^- X$ decays, where $D_s^- \to \phi\pi^-$ and $\phi \to K^+K^-$, an opposite-side flavour tagging algorithm, and an unbinned likelihood fit. Using the amplitude method an expected limit of 14.1 ps^{-1} is given and there is an observed lower limit of $\Delta m_s > 14.8$ ps^{-1} at the 95% C.L. At $\Delta m_s = 19$ ps^{-1}, the amplitude method yields a result that deviates from the hypothesis $\mathcal{A} = 0$ ($\mathcal{A} = 1$) by 2.5 (1.6) standard deviations, corresponding to a two-sided C.L. of 1% (10%). The likelihood curve is well behaved near a preferred value of 19 ps^{-1} with a 90% C.L. interval of $17 < \Delta m_s < 21$ ps^{-1}, assuming Gaussian uncertainties. Ensemble tests indicate that if Δm_s lies above the sensitive region, i.e., above approximately 22 ps^{-1}, there is a (5.0 ± 0.3)% probability that it would produce a likelihood minimum similar to the one observed in the interval $16 < \Delta m_s < 22$ ps^{-1}. This is the first report of a direct two-sided bound measured by a single experiment on the B_s^0 oscillation frequency, and places further constraints on the CKM unitarity triangle as is shown in Figure 5. This result is consistent with the subsequent observation of oscillations by the CDF experiment which measures a value $\Delta m_s = 17.31^{+0.33}_{-0.18}(\text{stat}) \pm 0.07(\text{syst})$ [14].

REFERENCES

1. V.M. Abazov *et al.* (DØ collaboration), Phys.Rev.Lett. **97** 97, 021802 (2006)
2. J. H. Christenson *et al.*, Phys. Rev. Lett. **13**, 138 (1964).
3. H. Albrecht *et al.*, (ARGUS Collaboration), Phys. Lett. **B192**, 245 (1987)
4. "B Physics at the Tevatron", arXiv:hep-ph/0201071.
5. J. Charles *et al.* (CKMfitter Group), Eur. Phys. J. **C41**, 1 (2005).
6. V.M. Abazov *et al.*, (DØ Collaboration) Fermilab-Pub-05/341-E, hep-physics/0507191, submitted to NIM-A.
7. S. Catani *et al.*, Phys. Lett. B **269**, 432 (1991), "Durham" jets with the p_T cut-off parameter set at 15 GeV/c.
8. J. Abdallah *et al.* (DELPHI Collaboration), Eur. Phys. J. C **32**, 185 (2004).
9. G. Borisov, Nucl. Instrum. Methods Phys. Res. Sect. A **417**, 384 (1998).
10. V. Abazov *et al.* (DØ Collaboration), Phys. Rev. D (to be published); DØ Note 5029, http://www-d0.fnal.gov/Run2Physics/WWW/results/prelim/B/B32/.
11. S.Eidelman *et al.*, Phys. Lett. B **592**, 1 (2004).
12. H.G. Moser and A. Roussarie, Nucl. Instrum. Methods Phys. Res. Sect. A **384**, 491 (1997).
13. CKMfitter Group (J. Charles et al.), Eur. Phys. J. C41, 1-131 (2005), [hep-ph/0406184], updated results and plots available at: http://ckmfitter.in2p3.fr
14. A. Abulencia [CDF - Run II Collaboration], arXiv:hep-ex/0606027.